2017. Proceedings of the Indiana Academy of Science 126(1):35–41

# INFRARED SPECTROSCOPIC STUDIES OF $C_{60}$ AND $C_{70}$ NANOPARTICLE INTERACTIONS WITH 2-PYRROLIDONE

**Joe L. Kirsch**[1], **Daniel Schemenauer** [2] and **Austin Engle**[2]: Department of Chemistry, Butler University, 4600 Sunset, Indianapolis, IN 46260 USA

**ABSTRACT**. Fourier transform infrared spectroscopy was used to investigate the interactions between $C_{60}$ and $C_{70}$ nanoparticles and 2-pyrrolidone (2-pyrrolidinone, $\gamma$–lactam) in a toluene solvent environment. Infrared spectra were collected for 2-pyrrolidone in toluene, 2-pyrrolidone in toluene saturated with $C_{60}$, and 2-pyrrolidone in toluene saturated with $C_{70}$ over a concentration range of 200 to 2 microliters ($\mu$L) of 2-pyrrolidone per mL of toluene or toluene saturated with the nanoparticles. At the higher concentrations of this range, small broadenings of the 2-pyrrolidone carbonyl stretching absorptions on the lower wavenumber side were observed when the 2-pyrrolidone was treated with $C_{60}$ and $C_{70}$. A significant shift was observed for the carbonyl absorption of 2-pyrrolidone when the 2-pyrrolidone was treated with $C_{60}$ at 5 and 2 $\mu$L of 2-pyrrolidone per mL of toluene saturated with $C_{60}$. These observed shifts suggest a 2-pyrrolidone–$C_{60}$ nanoparticle interaction or complex formation. A small broadening of the carbonyl absorption on the low wavenumber side was observed when the 2-pyrrolidone was treated with $C_{70}$ at 5 and 2 $\mu$L of 2-pyrrolidone per mL of toluene saturated with $C_{70}$. Spectral subtraction was used to reveal the carbonyl absorption for the 2-pyrrolidone–$C_{60}$ complex that exists at the higher concentration range, but is covered up by the intense absorption of the excess 2-pyrrolidone not interacting with $C_{60}$. The spectrum of 2-pyrrolidone in toluene (100 $\mu$L of 2-pyrrolidone per mL of toluene) was subtracted from the spectrum of 2-pyrrolidone in toluene saturated with $C_{60}$ (100 $\mu$L of 2-pyrrolidone per mL of toluene saturated with $C_{60}$). The subtraction process yielded a spectrum containing a spectral absorption very near the shifted absorption for 2-pyrrolidone treated with $C_{60}$ at the lower concentrations.

**Keywords:** Infrared spectroscopy, nanoparticles, $C_{60}$ and $C_{70,}$ fullerenes, fullerene/nanoparticle interactions, 2-pyrrolidone, 2-pyrrolidinone, $\gamma$-lactam

## INTRODUCTION

The interest in the interactions of $C_{60}$ and $C_{70}$ nanoparticles with a variety of molecular systems has motivated a number of studies using a variety of analysis methods (Holleman et al. 1999; Kyzyma et al. 2008; Jurow et al. 2012; King et al. 2012; Kyrey et al. 2012; Tropin et al. 2013; Bowles et al. 2014; Kirsch et al. 2015). This paper reports the results of an infrared spectroscopic study of the interactions between $C_{60}$ and $C_{70}$ nanoparticles and 2-pyrrolidone using toluene as a solvent environment (Aksenova et al. 2013).

The compound 2-pyrrolidone is a five-membered, cyclic amide sometimes referred to as gamma-lactam ($\gamma$-lactam) or 2-pyrrolidinone. There are a number of pharmaceutical and biological applications related to the 2-pyrrolidone cyclic structure (Midgley et al. 1992; Harreus et al. 2011). The $C_{60}$ and $C_{70}$ nanoparticles dissolve in aromatic solvents such as toluene to form colored solutions; $C_{60}$ in toluene is blue, while $C_{70}$ in toluene is red (Ruoff et al. 1993). Infrared spectroscopy was used in this study to seek shifts in the carbonyl absorption of the 2-pyrrolidone as an indication of its interactions with the $C_{60}$ and $C_{70}$ nanoparticles in a toluene solvent environment.

## EXPERIMENTAL METHODS

A Digilab FTS 7000 infrared spectrometer and a circle cell fitted with a ZnSe ATR rod were used to collect spectra for the investigation by averaging 500 scans at a spectral resolution of two wavenumbers. The empty circle cell was used as the background, single-beam spectrum for spectral collection. The spectrometer was purged with dry air for an hour prior to spectral collection to remove potentially interfering atmospheric water vapor. Since the 2-pyrrolidone interaction with the nanoparticles is likely an equilibrium process involving both interacting and non-interacting 2-pyrrolidone, spectral collection was carried out over a broad concentration range (200 to 2

---

[1] *Corresponding author:* Joe L. Kirsch, 317-940-9400 (phone), 317-940-8430 (fax), jkirsch@butler.edu.

[2] Undergraduate Student

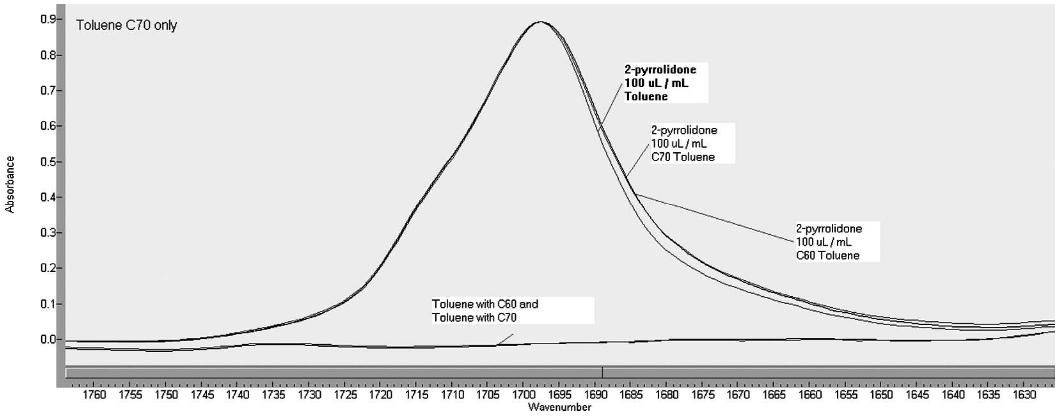

Figure 1.—The spectra of 100 μL of 2-pyrrolidone per mL of toluene, per mL of toluene saturated with $C_{60}$, and per mL of toluene saturated with $C_{70}$ are shown. In addition, the spectra of toluene saturated with $C_{60}$ and toluene saturated with $C_{70}$ are included.

microliters (μL) of 2-pyrrolidone per mL of toluene or toluene saturated with the nanoparticles) to determine the optimal concentrations to observe infrared spectral changes.

## INVESTIGATION RESULTS

Figure 1 contains the spectrum of 100 μL of 2-pyrrolidone per mL of toluene, the spectrum 100 μL of 2-pyrrolidone per mL of toluene saturated with $C_{60}$, and the spectrum of 100 μL of 2-pyrrolidone per mL of toluene saturated with $C_{70}$. In addition, the spectrum of toluene saturated with $C_{60}$ and the spectrum of toluene saturated with $C_{70}$ are shown. The spectra of toluene and toluene saturated with nanoparticles do not show any spectral absorption in the region of the 2-pyrrolidone carbonyl absorption. The spectra of the 2-pyrrolidone solutions containing $C_{60}$ and $C_{70}$ at these concentrations show a very small broadening of the carbonyl absorption on the low wavenumber side. While these broadenings are small, the broadenings were consistently observed in repeated experiments. Spectra collected at higher concentrations (200 μL of 2-pyrrolidone per mL of toluene and toluene saturated with $C_{60}$ or $C_{70}$) also show consistent, small broadening on the lower wavenumbers side of the carbonyl absorption of 2-pyrrolidone resulting from its nanoparticle treatment.

Complex formation, resulting from the interactions of the nanoparticles with the 2-pyrrolidone, is likely an equilibrium process involving both 2-pyrrolidone interacting and not interacting with the nanoparticles. Of course, shifting the equilibrium toward the 2-pyrrolidone–nanoparticle complex could result from increasing the concentration of either the nanoparticles or the 2-pyrrolidone. Changing the concentrations of the nanoparticles is limited by their low solubility in the toluene solvent, i.e., 2.8 mg of $C_{60}$ per mL of toluene (Ruoff et al. 1993). Increasing the concentration of 2-pyrrolidone would shift the equilibrium toward any 2-pyrrolidone–nanoparticle complex; however, it would also increase the amount of the 2-pyrrolidone not interacting with the nanoparticles which also contains the infrared probe, the carbonyl bond. The higher concentrations of the non-interacting 2-pyrrolidone could cover up the carbonyl absorption of any 2-pyrrolidone–nanoparticle complex and interfere with its observation.

Concentration studies were carried out to find an optimum concentration level of 2-pyrrolidone to generate a 2-pyrrolidone-nanoparticle complex and also allow the observation of the carbonyl absorption of the complex. Figure 2 shows spectra collected at 10 μL of 2-pyrrolidone per mL of toluene and toluene saturated with $C_{60}$ or $C_{70}$. The spectra show significant broadening of the carbonyl absorption of the 2-pyrrolidone treated with $C_{60}$, but only very slight broadening of the carbonyl absorption of 2-pyrrolidone treated with $C_{70}$ (Fig. 2).

Spectra collected at 5 and 2 μL of 2-pyrrolidone per mL of toluene and toluene saturated with $C_{60}$ or $C_{70}$ are shown in Fig. 3. Intensities of the absorptions have been adjusted to help clarify positioning along the wavenumber axis and do

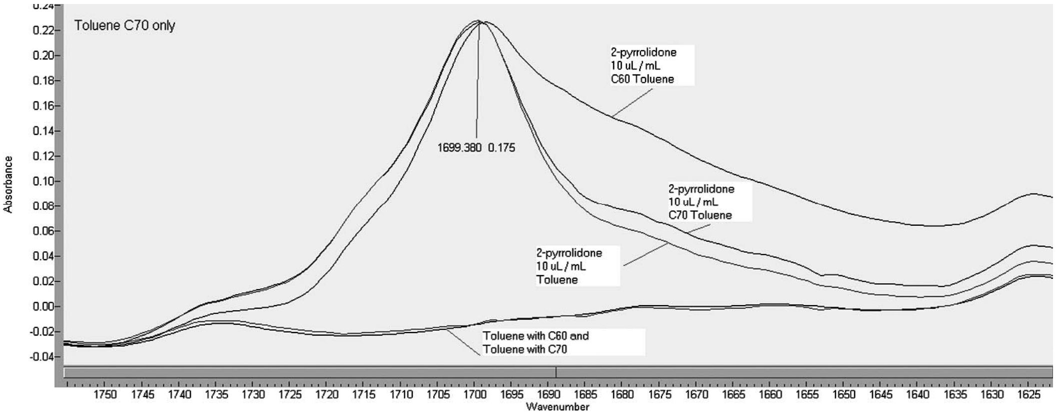

Figure 2.—The spectra of 10 μL of 2-pyrrolidone per mL of toluene, per mL of toluene saturated with $C_{60}$, and per mL of toluene saturated with $C_{70}$ are shown. In addition, the spectra of toluene saturated with $C_{60}$ and toluene saturated with $C_{70}$ are included.

not reflect relative concentrations of 2-pyrrolidone. Figure 3 shows spectra of 2-pyrrolidone with a significant shift of the whole carbonyl absorption from about 1700 $cm^{-1}$ to about 1687 $cm^{-1}$ resulting from its treatment with $C_{60}$ at 5 and 2 μL of 2-pyrrolidone per mL of toluene saturated with $C_{60}$. The significant shift of the 2-pyrrolidone, carbonyl absorption clearly supports a complex formation or interaction between the 2-pyrrolidone and $C_{60}$ nanoparticles. The spectrum of 2-pyrrolidone treated with $C_{70}$ shows only a very slight broadening of the carbonyl absorption on the low wavenumber side at 5 μl of 2-pyrrolidone per mL of toluene saturated with $C_{70}$.

Figure 4 shows four spectra collected over the concentration range of 10 to 5 μL of 2-pyrrolidone per mL of toluene saturated with $C_{60}$. The spectra show a clear transition of the absorption position of 2-pyrrolidone treated with the $C_{60}$ at 10 μL per mL (located near 1700 $cm^{-1}$) to its absorption at 5 μL per mL (located near 1687 $cm^{-1}$). Again, intensities of absorptions are adjusted to aid in seeing spectral absorption shifts along the wavenumber axis. The spectra suggests an absorption near 1700 $cm^{-1}$ for 2-pyrrolidone not interacting with $C_{60}$ and an absorption for 2-pyrrolidone interacting with $C_{60}$ near 1687 $cm^{-1}$ (Fig. 4).

The infrared absorption observed near 1687 $cm^{-1}$ for the complex formed between 2-pyrroli-

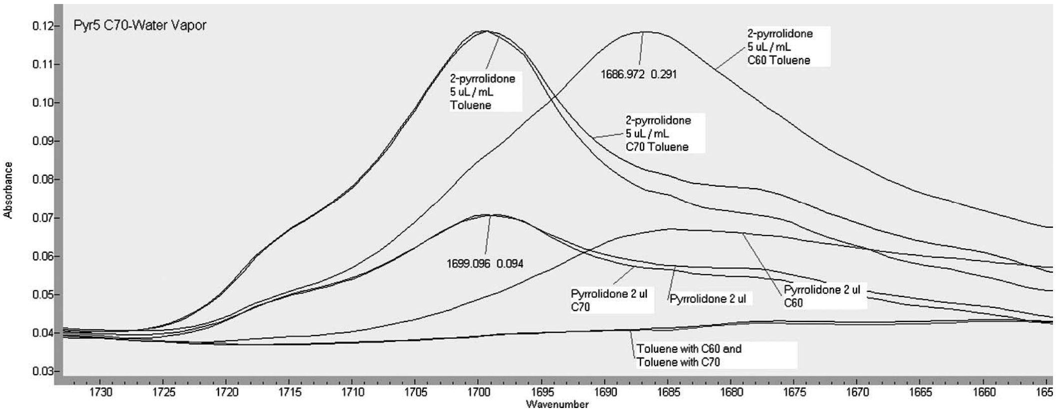

Figure 3.—The spectra of 5 and 2 μL of 2-pyrrolidone per mL of toluene, per mL of toluene saturated with $C_{60}$, and per mL of toluene saturated with $C_{70}$ are shown. In addition, the spectra of toluene saturated with $C_{60}$ and toluene saturated with $C_{70}$ are shown.

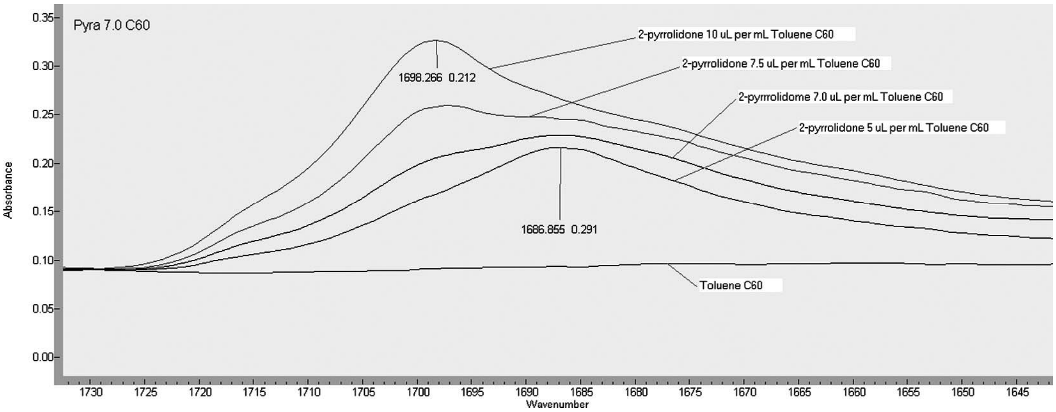

Figure 4.—The spectra of 10.0 µL, 7.5 µL, 7.0 µL, & 5.0 µL of 2-pyrrolidone per mL of toluene saturated with $C_{60}$ are shown to clarify the carbonyl shift from near 1698 $cm^{-1}$ to near 1687 $cm^{-1}$.

done and the $C_{60}$ nanoparticles at the lower concentrations (5 and 2 µL per mL) very likely exists at the higher concentrations of 2-pyrrolidone (200 and 100 µL per mL); however, this infrared absorption may be buried under the intense carbonyl absorption of the excess, non-interacting 2-pyrrolidone.

Spectral subtraction has been shown to be a useful tool in the separation of overlapping spectral absorptions resulting from a mixture of absorbing species (Gillette & Koenig 1984; Honigs et al. 1985; Charles 1994; Siyuan et al. 2010). Figure 5 contains again the spectrum of 100 and 5 µL of 2-pyrrolidone per ml of toluene and toluene saturated with $C_{60}$. The spectrum that results from subtracting the spectrum of 100 µL of 2-pyrrolidone per mL of toluene times 0.95 (subtraction factor) from the spectrum of 100 µL of 2-pyrrolidone per mL of toluene saturated with $C_{60}$ is also given in Fig. 5. The goal of the subtraction process is to remove the intense carbonyl absorption caused by the high concentration of the non-interacting 2-pyrrolidone at this high concentration level and thus to reveal the underlying carbonyl absorption of the relatively low concentration 2-pyrrolidone–$C_{60}$ complex. The result of the subtraction process yields a

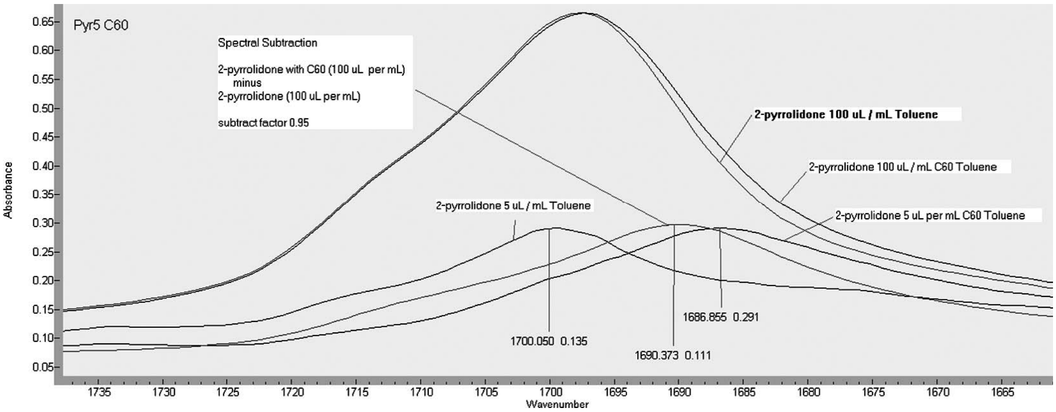

Figure 5.—The spectra of 100 µL of 2-pyrrolidone per mL of toluene, 100 µL of 2-pyrrolidone per mL of toluene saturated with $C_{60}$, 5 µL of 2-pyrrolidone per mL of toluene, and 5 µL of 2-pyrrolidone per mL of toluene saturated with $C_{60}$ are shown. Also shown is the spectrum that result from subtracting the spectrum of 100 µL of 2-pyrrolidone per mL of toluene from the spectrum of 100 µL of 2-pyrrolidone per mL of toluene saturated with $C_{60}$ (subtraction factor of 0.95).

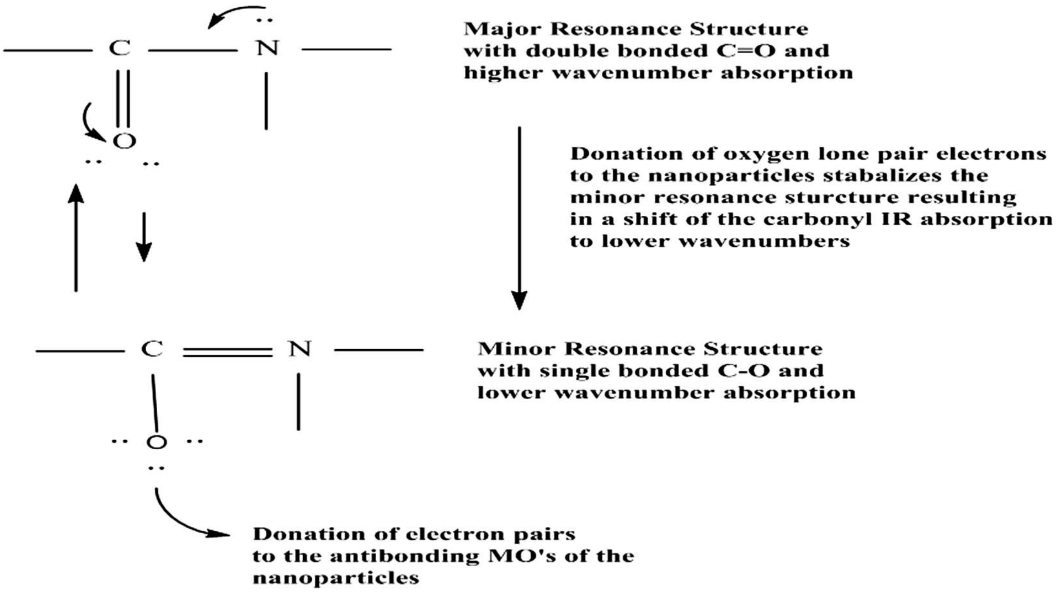

Figure 6.—A resonance structure model suggesting oxygen, lone pair donation to the nanoparticles ($C_{60}$) that shifts stability toward the resonance structure with the single bonded carbonyl and supports a shift of the carbonyl absorption to lower wavenumbers.

spectrum with a spectral absorption at 1690 $cm^{-1}$ which is in good agreement with the 1687 $cm^{-1}$ location of the absorption for the 2-pyrrolidone–$C_{60}$ complex observed in the spectrum at the lower concentration levels. Again, intensities of the absorptions have been adjusted to clarify positioning along the wavenumber axis.

## DISCUSSION AND CONCLUSIONS

The carbonyl infrared absorption in amide functionality is characterized by an absorption peak below 1700 $cm^{-1}$ compared to "normal" carbonyl absorption peaks observed above 1700 $cm^{-1}$. The traditional explanation for the carbonyl-absorptions of amides being below 1700 $cm^{-1}$ is that the lone-pair electrons on the nitrogen are delocalized into the amide carbon–nitrogen chemical bond generating a minor resonance structure with a carbon–oxygen single bond. This minor resonance structure adds single bond character to the carbonyl bond and contributes to the lower wavenumbers observed for the carbonyl infrared absorption in amide functionality (Avram & Mateescu 1970).

The observed shifts to lower wavenumbers of the carbonyl absorption in 2-pyrrolidone resulting from its interactions with $C_{60}$ could suggest that its interaction with the $C_{60}$ occurs through the lone-pair electrons of the oxygen part of its amide structure. A number of studies indicate that $C_{60}$ are good electron acceptors for molecular systems (Charvet et al. 2012; Schubert et al. 2013; Stranius et al. 2014). A recent study of the interactions of formamide with $C_{60}$ and $C_{70}$ showed a shift of the carbonyl absorption to higher wavenumbers suggesting an interaction through the nitrogen lone-pair electrons of the amide structure (Kirsch et al. 2015). The ring structure of the 2-pyrrolidone could make the nitrogen lone-pair electrons less accessible. If the lone pair electrons of the oxygen on the 2-pyrrolidone are donated into the antibonding molecular orbitals of the $C_{60}$ (Feng et al. 2008), the resonance structure containing the single bonded CO is stabilized yielding a lower wavenumber infrared absorption of the carbonyl group. Figure 6 shows this oxygen lone-pair donation process, and describes its impact on the carbonyl absorption.

In summary, the infrared spectra collected in this study suggest that interactions occur between 2-pyrrolidone and $C_{60}$ resulting from possible donation of the electron pairs from the oxygen part of its amide functionality into the antibonding MO's of the $C_{60}$. At lower concentrations of 2-pyrrolidone (5 and 2 μL of 2-pyrrolidone per mL of toluene and toluene saturated with $C_{60}$), a significant shift of its amide carbonyl absorption (~1700 $cm^{-1}$ to ~1687 $cm^{-1}$) is observed supporting this kind of interaction. A very slight broadening of the carbonyl absorption of 2-pyrrolidone when treated with $C_{70}$ in toluene suggests possible interactions, but further studies are needed to clarify. Spectral subtraction of 2-pyrrolidone from 2-pyrrolidone treated with $C_{60}$ at higher concentration levels of 2-pyrrolidone reveals an absorption in good agreement (1690 $cm^{-1}$ vs 1687 $cm^{-1}$) with that observed in the spectrum of the 2-pyrrolidone treated with $C_{60}$ at lower concentration and also supports complex formation with $C_{60}$.

## LITERATURE CITED

Aksenova, V.V., R.M. Nikonova, V.I. Lad'yanov, V.V. Mukhgalin & I.V. Sterkhova. 2013. IR-Fourier spectroscopic studies of structural changes in fullerenes $C_{60}$ and $C_{70}$–toluene systems. Russian Journal of Physical Chemistry 87:1002–1008.

Avram, M. & G. Mateescu. 1970. Infrared Spectroscopy, Chapter 8. John Wiley–Interscience, Hoboken, New Jersey. 439 pp.

Bowles, F.L., M.M. Olmstead & A.L. Balch. 2014. Preparation and crystallographic characterization of C60{η1-Ru(CO)2(η5-C5H5)}2: a locally crowded organometallic fullerene without the usual η2-bonding. Journal of American Chemical Society 136:3338–3341.

Charles, Y. 1994. Identification of chemical contamination on a rayon yarn using extraction and infrared spectral subtraction. Industrial and Engineering Chemistry Research 33:2836–2839.

Charvet, R., Y. Yamamoto, T. Sasaki, J. Kim, K. Kato, M. Takata, A. Saeki, S. Seki & T. Aida. 2012. Segregated and alternately stacked donor/acceptor nanodomains in tubular morphology tailored with zinc porphyrin–$C_{60}$ amphiphilic dyads: clear geometrical effects on photoconduction. Journal of the American Chemical Society 134:2524–2527.

Feng, M., J. Zhao & H. Petek. 2008. Atomlike, hollow-core-bound molecular orbitals of $C_{60}$. Science 320:359–362.

Gillette, P. & J. Koenig. 1984. Objective criteria for absorbance subtraction. Applied Spectroscopy 38:334–337.

Harreus, A.L., R. Backes, J.O. Eichler, R. Feuerhake, C. Jakel, U. Mahn, R. Pinkos & R. Vogelsand. 2011. Ullmann's Encyclopedia of Industrial Chemistry. Wiley-VCH, Weinheim, Germany. Version of Record online: 15 OCT 2011 | DOI: 10.1002/14356007.a22_457.pub2.

Holleman, I., G. von Heiden & A. van der Avoird. 1999. An infrared study on CO intercalated in solid $C_{60}$. Journal of Chemical Physics 110:2129–2139.

Honigs, D., G. Hieftje, H. Mark & T. Hirschfeld. 1985. Unique-sample selection via near-infrared spectral subtraction. Analytical Chemistry 57:2299–2303.

Jurow, M., C. Farley, C. Pabon, B. Hageman, A. Dolor & C.M. Drain. 2012. Facile synthesis of a flexible tethered porphyrin dimer that preferentially complexes fullerene $C_{70}$. Chemical Communications (Cambridge, United Kingdom) 48:4731–4733.

King, B.T., M.M. Olmstead, K.K. Baldridge, B. Kumar, A.L. Balch & J.A. Gharamaleki. 2012. Molecular nesting in co-crystals of tetrabenzoquadrannulene and $C_{60}$: application of the sphere in a cone model. Chemical Communications (Cambridge, United Kingdom) 48:9882–9884.

Kirsch, J.L., E. Brown, J. Kanter & J. Wade. 2015. Infrared investigations of $C_{60}$ and $C_{70}$ nanoparticle interactions with the amide functionality in formamide. Proceedings of the Indiana Academy of Science 124:1–7.

Kyrey, T.O., O.A. Kyzyma, M.V. Avdeev, T.V. Tropin, M.V. Korobov, V.L. Aksenov & L.A. Bulavin. 2012. Absorption characteristics of fullerene $C_{60}$ in N-methyl-2-pirrolidone/toluene mixtures. Fullerenes, Nanotubes, and Carbon Nanostructures 20:341–344.

Kyzyma, O.A., L.A. Bulavin, V.L. Aksenov, T.V. Tropin, M.V. Avdeev, M.V. Korobov, S.V. Snegir & L. Rosta. 2008. Aggregation in $C_{60}$/NMP, $C_{60}$/NMP/water and $C_{60}$/NMP/Toluene Mixtures. Fullerenes, Nanotubes, and Carbon Nanostructures 16:610–615.

Midgley, I., A.J. Hood, L.F. Chasseaud, C.J. Brindley, S. Baughman & G. Allan. 1992. Percutaneous absorption of co-administered N-methyl-2-[$^{14}$C]pyrrolidinone and 2-[$^{14}$C]pyrrolidinone in the rat. Food and Chemical Toxicology 30:57–64.

Ruoff, R.S., D.S. Tse, W. Malhotra & D.C. Lorents. 1993. Solubilities of $C_{60}$ in a variety of solvents. Journal of Physical Chemistry 97:3379–3383.

Schubert, C., M. Wielopolski, L.H. Mewes, R.G. de Miguel, C. van der Pol, K.C. Moss, M.R. Bryce, J.E. Moser, T. Clark & D.M. Guldi. 2013. Precise control of intramolecular charge-transport: the interplay of distance and conformational effects. Chemistry (Weinheim an der Bergstrasse, Germany) 19:7575–7586.

Siyuan, L., Z. Yongsheng, Z. Yan, H. Weilin, H. Kaisheng, J. Ming, C. Zehong & Z. Jiewei. 2010. Application of infrared spectral subtraction method to rapid qualitative identification of fabric coating. Guangdong Huagong 37:181–182.

Stranius, K., V. Iashin, T. Nikkonen, M. Muuronen, J. Helaja & N. Tkachenko. 2014. Effect of mutual position of electron donor and acceptor on photoinduced electron transfer in supramolecular chlorophyll-fullerene dyads. Journal of Physical Chemistry A 118:1420–1429.

Tropin, T.V., T.O. Kyrey, O.A. Kyzyma, A.V. Feoktistov, M.V. Avdeev, L.A. Bulavin, L. Rosta & V.L. Aksenov. 2013. Experimental investigation of $C_{60}$/NMP/toluene solutions by UV-Vis spectroscopy and small-angle neutron scattering. Journal of Surface Investigation: X-Ray, Synchrotron and Neutron Techniques 7: 1–4.

*Manuscript received 10 February 2017, revised 10 July 2017.*